

Limits and correlations of T and Z components of CPT -odd coefficients of the Standard Model Extension at DUNE

Luis A. Delgadillo,^{1,2,*} O. G. Miranda,^{3,†} G. Moreno-Granados,^{3,4,‡} and C. A. Moura^{5,§}

¹*Departamento de Física, Escuela Superior de Física
y Matemáticas del Instituto Politécnico Nacional,*

Unidad Adolfo López Mateos, Edificio 9, 07738 Ciudad de México, Mexico

²*Institute of High Energy Physics, Chinese Academy of Sciences, Beijing 100049, China*

³*Departamento de Física, Centro de Investigación y de Estudios*

Avanzados del IPN Apdo. Postal 14-740 07000 Ciudad de México, Mexico

⁴*Center for Neutrino Physics, Virginia Tech, Blacksburg, VA, 24061, USA*

⁵*Centro de Ciências Naturais e Humanas,*

Universidade Federal do ABC - UFABC, Av. dos Estados,

5001, 09210-580, Santo André-SP, Brazil

(Dated: September 6, 2024)

We consider the possible effect of the Standard Model Extension (SME) coefficient $(a_L)^Z$ in the neutrino propagation and discuss how this can affect DUNE limits on the coefficient $(a_L)^T$ found elsewhere. Based on an analysis that considers both coefficients, we find new constraints for them coming from a DUNE-like experiment. Furthermore, we investigate the correlations of the standard oscillation parameters, the leptonic CP -violating phase, δ_{CP} , and the atmospheric mixing angle, $\sin^2 \theta_{23}$, with respect to the SME coefficients $(a_L)^T$ and $(a_L)^Z$.

I. INTRODUCTION

On the neutrino oscillation frontier, where nearly all of the available data is compatible with the standard three-flavor oscillation paradigm, precision measurements can be performed to investigate Beyond Standard Model (BSM) physics that may disturb the oscil-

* ldelgadillof2100@alumno.ipn.mx

† omar.miranda@cinvestav.mx

‡ guadalupe.moreno@cinvestav.mx

§ celio.moura@ufabc.edu.br

lation pattern. Looking for perturbations on the neutrino oscillation standard model brings new opportunities to access, for example, the Planck scale.

In the three neutrino oscillation picture, NOvA [1, 2], T2K [3, 4], and recently IceCube [5] collaborations are leading the precision measurements on both the atmospheric oscillation parameters, Δm_{32}^2 and $\sin^2 \theta_{23}$, and the CP -violating phase, δ_{CP} [3]. The current measurement of the angle θ_{23} demonstrates consistency with maximal mixing (i.e., $\theta_{23} = \pi/4$).

This has implications for our understanding of neutrino masses and the nature of neutrino flavor mixing. Furthermore, the precise determination of $\sin^2 \theta_{23}$ is crucial for refining our understanding of the neutrino mass hierarchy, the ordering of neutrino mass eigenstates, and for probing possible sources of CP violation in the neutrino sector.

On the other hand, accurately determining δ_{CP} is a primary goal of several ongoing and planned long-baseline neutrino oscillation experiments. Present-day measurements of δ_{CP} have been reported, mainly by NOvA and T2K collaborations. Their results seem to differ, and might be a challenge to interpret them if this difference persists in the future. While the NOvA collaboration best-fit agrees with a value of $\delta_{CP} \simeq 0.8\pi$ [1], a similar analysis from the T2K collaboration reports $\delta_{CP} \simeq 1.4\pi$ [3], under the neutrino mass Normal Ordering (NO). A recent joint oscillation analysis of the Super-Kamiokande and T2K collaborations is consistent with a best-fit value of $\delta_{CP} \simeq 1.4\pi$ [6]. Nevertheless, some proposals to alleviate such discrepancy on the measurement of δ_{CP} include: neutrino Non-Standard Interactions (NSI) [7–9] and sterile neutrinos [10, 11], among other BSM scenarios [12].

The Standard Model of particle physics (SM) is thought to represent a low-energy effective gauge theory of a more fundamental theory in which the Planck scale ($M_{Pl} \sim 10^{28}$ eV) would be the natural mass scale. Likewise, the Standard Model Extension (SME) framework [13] parameterizes the possible breakdowns of the Lorentz and CPT symmetries that might arise from a fundamental theory that incorporates both, the gravitational force from one side, and the strong, weak, and electromagnetic interactions of the SM from the other side. Such potential violations of the CPT and Lorentz symmetries may arise at very high energies, well above the electroweak scale, for instance, within the context of string theory [14–17]. Furthermore, it has been argued that potential Lorentz Invariance Violation (LIV) and CPT symmetry breakdown in the neutrino sector might result from neutrino NSI with scalar fields [18–29].

For reviews regarding CPT violation and LIV in the neutrino sector, see, e.g., Refs. [30–

35]. As far as neutrino oscillation experiments are concerned, CPT violation in the neutrino sector was suggested in order to explain the Liquid Scintillator Neutrino Detector (LSND) and MiniBooNE anomalies [36–41]. For studies regarding possible LIV and CPT -violating effects in various neutrino oscillation experiments, we refer to [42–70]. Moreover, non-oscillatory probes of Lorentz and CPT breakdowns in the neutrino sector include: beta decay [71–73], double beta decay [74, 75], and cosmic neutrino background [76].

In this paper, we examine the particular BSM case of potential violations of Lorentz invariance and CPT symmetries within the context of accelerator-based long-baseline neutrino oscillation experiments, such as the Deep Underground Neutrino Experiment (DUNE) [77], a next-generation long-baseline neutrino oscillation experiment. Long-baseline neutrino experiments have sensitivity to CPT symmetry and Lorentz invariance violations through SME coefficients proportional to their baseline. One can see this through the oscillation probability expression, which can be parameterized as [78],

$$P_{\nu_\beta \rightarrow \nu_\alpha}^{(1)} = 2L(P_C^{(1)})_{\alpha\beta}, \quad (1)$$

where L is the baseline and

$$(P_C^{(1)})_{\alpha\beta} = \text{Im}((S_{\alpha\beta}^{(0)})^*(C^{(1)})_{\alpha\beta}). \quad (2)$$

In Eq. (2),

$$|(S_{\alpha\beta}^{(0)})|^2 = P_{\nu_\beta \rightarrow \nu_\alpha}^{(0)}, \quad (3)$$

is the standard three neutrino flavor oscillation probability. Considering only the CPT -odd coefficients $(\tilde{a}_L)_{\alpha\beta}^A$, for $A = T, Z$ and $\alpha, \beta = e, \mu, \tau$:

$$(C^{(1)})_{\alpha\beta} = (\tilde{a}_L)_{\alpha\beta}^T - \hat{N}^Z (\tilde{a}_L)_{\alpha\beta}^Z, \quad (4)$$

where

$$\hat{N}^Z = -\sin \chi \sin \theta \cos \phi + \cos \chi \cos \theta, \quad (5)$$

is the Z component of the vector representing the neutrino propagation direction in the Sun-centered frame in terms of local spherical coordinates at the detector (see Fig. 2 of Ref. [79] for an illustration). In Eq. (5), χ is the colatitude of the detector, θ is the angle at the detector between the beam direction and vertical, and ϕ the angle between the beam and east of south. Notice that we are not taking into account sidereal variations so the

components $A = X, Y$ of $(\tilde{a}_L)_{\alpha\beta}^A$ are not relevant. The aim of this work is to investigate the consequences of the possible coexistence of the time (T) and spatial (Z) components of the CPT -odd coefficients of the SME.

II. EXPERIMENTAL CONTEXT AND THEORETICAL FRAMEWORK

Long-baseline neutrino oscillation experiments are crucial for solving puzzles in the conventional three-neutrino paradigm as well as investigating different new physics scenarios, such as possible breakdowns of the Lorentz and CPT symmetries. In recent neutrino oscillation analyzes [54, 57, 61, 65], the possible violation of CPT symmetry, that would imply violation of the Lorentz invariance principle, was studied in the framework of the SME, in such a way that CPT -odd coefficients can have their time-component constrained through the neutrino propagation in long baseline experiments. However, from equations (1)-(4), we see that if the Z -component of the same coefficient is considered in the analysis, a correlation arises between them which affects the predicted limits on the time component alone.

We introduced the SME phenomenology of CPT symmetry violation and LIV through the coefficients $(\tilde{a}_L)_{\alpha\beta}^A$ found in Eq. (4) as part of the oscillation probability. Henceforth, we will focus on the Hamiltonian picture of neutrino propagation, which is directly related to our computing methodology explained in the next section, Section III. We describe the neutrino propagation from the source to the detector considering the Hamiltonian containing three components,

$$\hat{H} = \hat{H}_{\text{vacuum}} + \hat{H}_{\text{matter}} + \hat{H}_{\text{LIV}}, \quad (6)$$

where \hat{H}_{vacuum} describes the neutrino propagation in vacuum, \hat{H}_{matter} contains the Mikheyev-Smirnov-Wolfenstein (MSW) matter potential, and \hat{H}_{LIV} includes the perturbative effects from LIV and possibly CPT symmetry violation. Explicitly, considering only the relevant CPT -odd coefficients of the SME neutrino sector:

$$\hat{H}_{\text{LIV}} = \begin{pmatrix} a_{ee} & a_{e\mu} & a_{e\tau} \\ a_{e\mu}^* & a_{\mu\mu} & a_{\mu\tau} \\ a_{e\tau}^* & a_{\mu\tau}^* & a_{\tau\tau} \end{pmatrix} - \hat{N}^Z \begin{pmatrix} a_{ee}^Z & a_{e\mu}^Z & a_{e\tau}^Z \\ a_{e\mu}^{Z*} & a_{\mu\mu}^Z & a_{\mu\tau}^Z \\ a_{e\tau}^{Z*} & a_{\mu\tau}^{Z*} & a_{\tau\tau}^Z \end{pmatrix}, \quad (7)$$

where $a_{\alpha\beta}$ represent the time component and $a_{\alpha\beta}^Z$ the Z -spatial component of the coefficients

for each neutrino oscillation channel ($\alpha, \beta = e, \mu, \tau$). From now on, we neglect the script T from the time component and simplify the notation so that $(a_L)_{\alpha\beta}^T = a_{\alpha\beta}$ and $(a_L)_{\alpha\beta}^Z = a_{\alpha\beta}^Z$.

III. METHODOLOGY

In this study, we use GLoBES [80, 81] and its additional NSI plugin *snu.c* [82, 83] which was modified to implement the CPT -odd SME coefficients at the Hamiltonian. Moreover, to simulate a DUNE-like experimental configuration, we use the available DUNE configuration ancillary files [84] for GLoBES and specifications from DUNE technical design report (TDR) [77, 85, 86], where can be found more details and information on the experiment. DUNE will consist of up to four modules, each containing approximately 10 kton liquid argon detectors, with a mean neutrino energy around 2.5 GeV, located at 1285 km from the beam source (on-axis) with a 1.2 MW power in the first phase of operations. We consider a time exposure of 10 years, evenly distributed between neutrino and antineutrino modes.

We employ a minimum square analysis to quantify the statistical significance to CPT -odd SME coefficients, using both neutrino and antineutrino data sets. The total χ^2 -function is given as [9]

$$\chi^2 = \sum_{\ell} \tilde{\chi}_{\ell}^2 + \chi_{\text{prior}}^2, \quad (8)$$

where the corresponding $\tilde{\chi}_{\ell}^2$ -function stands for each channel ℓ , with $\ell = (\nu_{\mu}(\bar{\nu}_{\mu}) \rightarrow \nu_e(\bar{\nu}_e), \nu_{\mu}(\bar{\nu}_{\mu}) \rightarrow \nu_{\mu}(\bar{\nu}_{\mu}))$, and is provided as in Ref. [87]

$$\tilde{\chi}_{\ell}^2 = \min_{\xi_j} \left[\sum_i^{n_{\text{bin}}} 2 \left\{ N_{i,\text{test}}^{3\nu+\text{LIV}}(\Omega, \Theta, \{\xi_j\}) - N_{i,\text{true}}^{3\nu} + N_{i,\text{true}}^{3\nu} \log \frac{N_{i,\text{true}}^{3\nu}}{N_{i,\text{test}}^{3\nu+\text{LIV}}(\Omega, \Theta, \{\xi_j\})} \right\} + \sum_j^{n_{\text{syst}}} \left(\frac{\xi_j}{\sigma_j} \right)^2 \right], \quad (9)$$

where $N_{i,\text{true}}^{3\nu}$ are the simulated events at the i -th energy bin, considering the standard three neutrino oscillations framework, $N_{i,\text{test}}^{3\nu+\text{LIV}}(\Omega, \Theta, \{\xi_j\})$ are the computed events at the i -th energy bin including CPT -odd SME coefficients (one parameter at a time). In addition, $\Omega = \{\theta_{12}, \theta_{13}, \theta_{23}, \delta_{CP}, \Delta m_{21}^2, \Delta m_{31}^2\}$ is the set of neutrino oscillation parameters, while $\Theta = \{|a_{\alpha\beta}|, \phi_{\alpha\beta}, a_{\alpha\alpha}, \dots\}$ is the set of either isotropic, $a_{\alpha\beta}$, or Z -spatial, $a_{\alpha\beta}^Z$, SME coefficients, and $\{\xi_j\}$ are the nuisance parameters to account for the systematic uncertainties. Moreover, σ_j are the systematic uncertainties as reported in the DUNE TDR [86]. To obtain our

simulated events, we consider the neutrino oscillation parameters from Salas *et al.* [88] as *true* values, shown in Table I.

Oscillation parameter best fit NO	
θ_{12}	34.3°
θ_{23}	49.26°
θ_{13}	8.53°
Δm_{21}^2 [10^{-5} eV ²]	7.5
$ \Delta m_{31}^2 $ [10^{-3} eV ²]	2.55
δ_{CP}/π	1.08

TABLE I: Standard oscillation parameters used in our analysis [88]. We consider the NO throughout this study.

Furthermore, the implementation of external input for the standard oscillation parameters on the χ^2 function is performed via Gaussian priors [87]

$$\chi_{\text{prior}}^2 = \sum_k^{n_{\text{priors}}} \frac{(\Omega_{k,\text{true}} - \Omega_{k,\text{test}})^2}{\sigma_k^2}. \quad (10)$$

The central values of the oscillation parameter priors, $\Omega_{k,\text{true}}$, are fixed to their best-fit value from Ref. [88], considering NO and σ_k corresponding to the 68.27% confidence level (C.L.) for each parameter k .

IV. RESULTS AND DISCUSSIONS

In this section, we present our results of the projected limits and sensitivities to the *CPT*-odd SME coefficients $a_{\alpha\beta}$ and $a_{\alpha\beta}^Z$ at a DUNE-like experimental configuration.

First, we examine the correlations among the SME coefficients $a_{\alpha\beta}$ and $a_{\alpha\beta}^Z$. The correlation between the time and the *Z*-component of the *CPT*-odd coefficients for DUNE is depicted in Fig. 1. Because the *Z*-component is proportional to \hat{N}^Z , which is relatively small for the DUNE location ($\hat{N}^Z \simeq 0.16$), constraints on the time component are stronger in this case. We obtain \hat{N}^Z from the values of the angles relative to the DUNE location found in Table II, Appendix A.

Second, in Figs. 2 and 3, we examine the correlations of the coefficients $a_{\alpha\beta}$ and $a_{\alpha\beta}^Z$ with δ_{CP} . Moreover, we assess the impact of the flavor-changing $a_{\alpha\beta}$ and $a_{\alpha\beta}^Z$ on the future determination of δ_{CP} . A robust measurement of δ_{CP} can be accomplished even in the presence of Lorentz violating effects, as shown in Fig. 4. The correlations of $a_{\alpha\beta}$ and $a_{\alpha\beta}^Z$ with $\sin^2 \theta_{23}$ are presented in Figs. 5 and 6. Just as importantly, the LIV phases, $\phi_{\alpha\beta}$ and $\phi_{\alpha\beta}^Z$, might compromise the determination of δ_{CP} , and similarly for the atmospheric mixing angle, θ_{23} [63]. In Fig. 7, we show the projected sensitivities to the isotropic coefficients $a_{\alpha\beta}$, as well as the anisotropic Z -spatial coefficients $a_{\alpha\beta}^Z$. Finally, in Fig. 8, we display the correlations of the LIV phases, $\phi_{\alpha\beta}$ and $\phi_{\alpha\beta}^Z$, with respect to δ_{CP} .

A. Correlations of time and Z -spatial components the CPT -odd SME coefficients

Previous assessments on the isotropic SME coefficients $a_{\alpha\beta}$ considered $a_{\alpha\beta}^Z = 0$ [50, 54, 55, 57, 63]. However, in this paper, we consider the possibility of correlations between $a_{\alpha\beta}$ and $a_{\alpha\beta}^Z$.

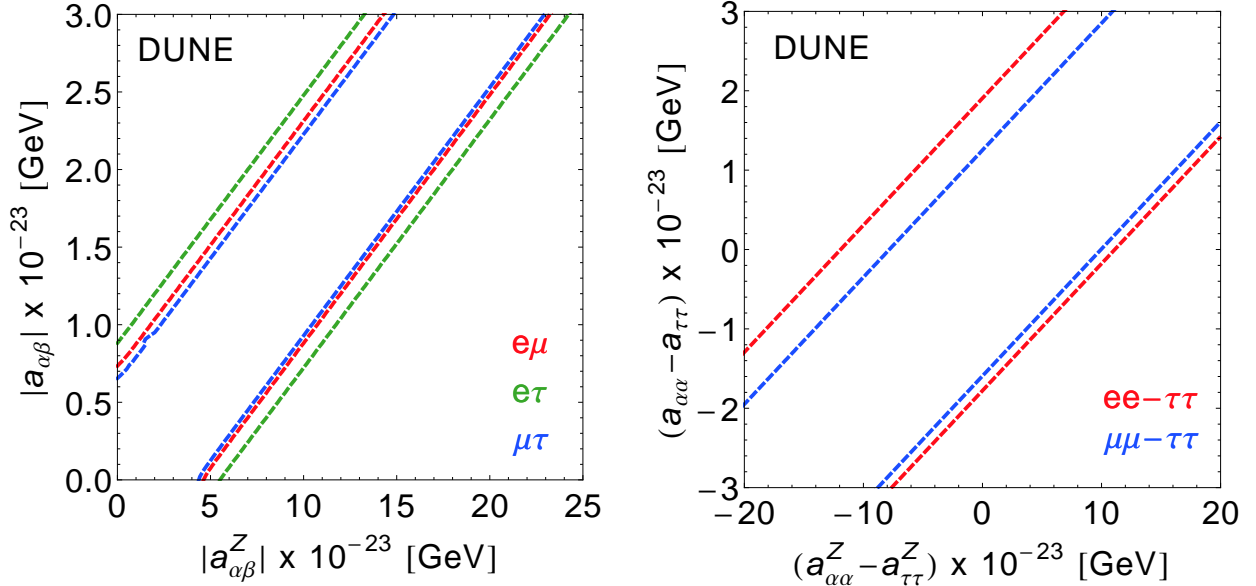


FIG. 1: Expected 95% C.L. sensitivity regions in the $|a_{\alpha\beta}|$ vs. $|a_{\alpha\beta}^Z|$ and $(a_{\alpha\alpha} - a_{\tau\tau})$ vs. $(a_{\alpha\alpha}^Z - a_{\tau\tau}^Z)$ projection planes, respectively. In the left panel, the (red, green, blue)-dashed lines correspond to the SME coefficients from the $\alpha\beta = (e\mu, e\tau, \mu\tau)$ channels. We have marginalized over the corresponding LIV phases, $\phi_{\alpha\beta}$ and $\phi_{\alpha\beta}^Z$, in the interval $[0-2\pi]$. In the right panel, $\alpha\alpha = (ee, \mu\mu)$, respectively, for red and blue colors. We marginalize over θ_{23} and δ_{CP} around their 1σ uncertainty [88]. All the remaining oscillation parameters are fixed to their NO best fit values. See text for a detailed explanation.

In Fig. 1, we display in dashed lines the expected 95% C.L. sensitivity regions in the $|a_{\alpha\beta}|$ vs. $|a_{\alpha\beta}^Z|$ and $(a_{\alpha\alpha} - a_{\tau\tau})$ vs. $(a_{\alpha\alpha}^Z - a_{\tau\tau}^Z)$ projection planes, respectively on the left and right panels. The projected 95% C.L. sensitivities to the isotropic non-diagonal SME coefficients are $|a_{e\tau}| \lesssim 0.92 \times 10^{-23}$ GeV ($|a_{e\tau}^Z| = 0$), $|a_{e\mu}| \lesssim 0.75 \times 10^{-23}$ GeV ($|a_{e\mu}^Z| = 0$), and $|a_{\mu\tau}| \lesssim 0.68 \times 10^{-23}$ GeV ($|a_{\mu\tau}^Z| = 0$), accordingly. However, existing bounds on the isotropic SME coefficients from the Super-Kamiokande experiment set $|a_{e\tau}| < 2.8 \times 10^{-23}$ GeV, $|a_{e\mu}| < 1.8 \times 10^{-23}$ GeV, and $|a_{\mu\tau}| < 5.1 \times 10^{-24}$ GeV [47]; all bounds at 95% C.L. Hence, a DUNE-like experimental configuration could improve the limits set on the isotropic SME coefficients $|a_{e\mu}|$ and $|a_{e\tau}|$ with respect to those from Super-Kamiokande.

B. Correlations of the SME coefficients with δ_{CP}

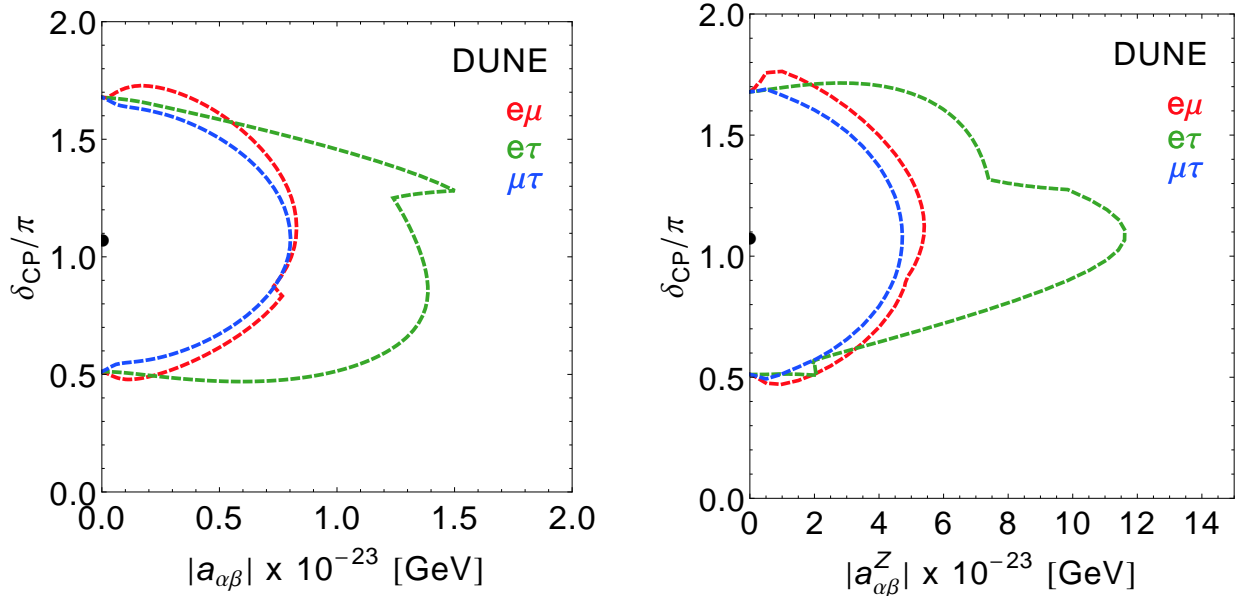


FIG. 2: The expected 95% C.L. sensitivity regions in the left panel $|a_{\alpha\beta}| - \delta_{CP}$ and in the right panel $|a_{\alpha\beta}^Z| - \delta_{CP}$ projection plane. The (red, green, blue)-dashed lines correspond to the SME coefficients from the $\alpha\beta = (e\mu, e\tau, \mu\tau)$ channels, respectively. We have marginalized over θ_{23} around its 1σ uncertainty [88], and corresponding LIV phases, $\phi_{\alpha\beta}$ and $\phi_{\alpha\beta}^Z$, free within $[0-2\pi]$. All the remaining oscillation parameters are fixed to their NO best fit values. See text for a detailed explanation.

The correlations among δ_{CP} and the off-diagonal SME coefficients, $|a_{\alpha\beta}|$ and $|a_{\alpha\beta}^Z|$, are displayed in Fig. 2. In both situations, we have marginalized over the atmospheric mixing angle, θ_{23} , around its 1σ uncertainty [88], as well as the CPT -odd phases, $\phi_{\alpha\beta}$ and $\phi_{\alpha\beta}^Z$, in the interval $[0-2\pi]$. Furthermore, we find that the presence of the flavor-changing $(e - \mu)$ and $(e - \tau)$ channels have a greater impact on the determination of δ_{CP} .

Regarding the diagonal SME coefficients, taking advantage of the freedom to redefine the diagonal elements up to a global constant, we conduct an analysis of the elements $a_{\alpha\alpha} - a_{\tau\tau}$ and $a_{\alpha\alpha}^Z - a_{\tau\tau}^Z$. The correlations with respect to δ_{CP} and $\sin^2 \theta_{23}$ are shown in Figs. 3 and 6, accordingly.

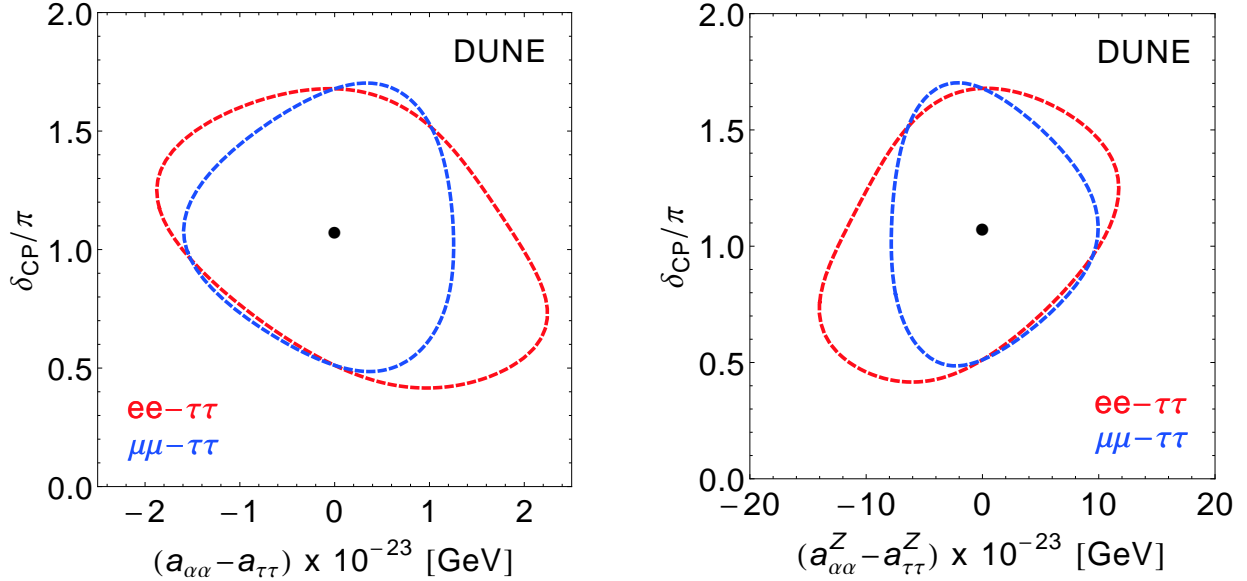


FIG. 3: Expected 95% C.L. sensitivity regions in the left panel $(a_{\alpha\alpha} - a_{\tau\tau}) - \delta_{CP}$ and in the right panel $(a_{\alpha\alpha}^Z - a_{\tau\tau}^Z) - \delta_{CP}$ projection plane. The (red, blue)-dashed lines correspond to $\alpha\alpha = (ee, \mu\mu)$, respectively. We have marginalized over θ_{23} around its 1σ uncertainty [88]. All the remaining oscillation parameters are fixed to their NO best fit value. See text for a detailed explanation.

In Fig. 3, we display our results of the projected 95% C.L. sensitivity regions $(a_{\alpha\alpha} - a_{\tau\tau}) - \delta_{CP}$ (left panel) and $(a_{\alpha\alpha}^Z - a_{\tau\tau}^Z) - \delta_{CP}$ (right panel). We notice that the determination of δ_{CP} is more affected by the coefficients $a_{ee} - a_{\tau\tau}$ and $a_{ee}^Z - a_{\tau\tau}^Z$ than it is by the $\mu\mu - \tau\tau$ coefficients. Here, we have marginalized over the atmospheric mixing angle θ_{23} around its 1σ uncertainty [88]. Besides, all the remaining oscillation parameters were fixed to their best-fit values from Table I.

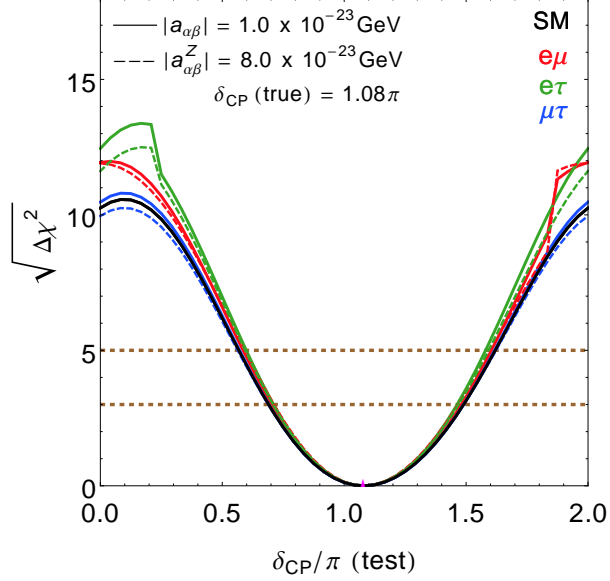


FIG. 4: The expected leptonic CP -phase precision sensitivity at DUNE. The (red, green, blue) lines correspond to the inclusion of non-zero SME coefficients from the $\alpha\beta = (e\mu, e\tau, \mu\tau)$ channels, respectively. The black line represents the standard three neutrino oscillation picture. The brown dashed horizontal lines display the 3σ and 5σ C.L. We marginalize over θ_{23} around its 1σ uncertainty [88], and corresponding LIV phases $\phi_{\alpha\beta}$ and $\phi_{\alpha\beta}^Z$ in the interval $[0-2\pi]$. The magnitude of the non-diagonal SME coefficients is fixed ($|a_{\alpha\beta}| = 1.0 \times 10^{-23}$ GeV, $|a_{\alpha\beta}^Z| = 8.0 \times 10^{-23}$ GeV). All the remaining oscillation parameters are fixed to their NO best fit value. See text for details.

In Fig. 4, we show the precision sensitivity to the leptonic CP -phase in the presence of LIV. We observe that the precision sensitivity of δ_{CP} is modified, at high significance ($\sqrt{\Delta\chi^2} \gtrsim 7\sigma$ C.L.), by the inclusion of non-zero SME coefficients ($|a_{\alpha\beta}|$ or $|a_{\alpha\beta}^Z|$) from the off-diagonal ($e - \mu$) and ($e - \tau$) channels, while remaining practically unchanged by the presence of the ($\mu - \tau$) channel. Hence, a robust measurement of δ_{CP} can be accomplished even in the presence of Lorentz violating effects from the non-diagonal channels.

C. Correlations of the SME coefficients with $\sin^2 \theta_{23}$

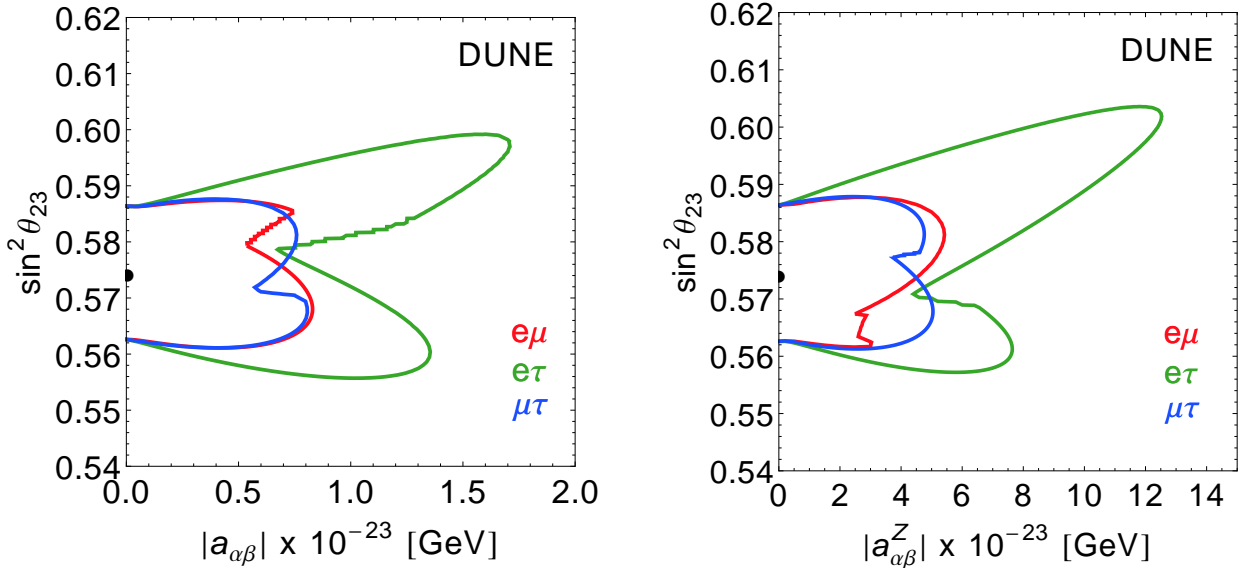


FIG. 5: Expected 95% C.L. sensitivity regions in the $(|a_{\alpha\beta}|, |a_{\alpha\beta}^Z|) - \sin^2 \theta_{23}$ projection plane. The (red, green, blue)-solid lines correspond to the SME coefficients from the $\alpha\beta = (e\mu, e\tau, \mu\tau)$ channels, respectively. We have marginalized over δ_{CP} around its 1σ uncertainty [88], and corresponding LIV phases, $\phi_{\alpha\beta}$ and $\phi_{\alpha\beta}^Z$, from $[0-2\pi]$. All the remaining oscillation parameters were fixed to their NO best fit values. See text for a detailed explanation.

In Fig. 5, we show the correlations between the off-diagonal SME coefficients, $|a_{\alpha\beta}|$ and $|a_{\alpha\beta}^Z|$, with the atmospheric mixing angle, $\sin^2 \theta_{23}$. In this case, we marginalized over δ_{CP} around its 1σ uncertainty [88], as well as corresponding CPT -odd phases, $\phi_{\alpha\beta}$ and $\phi_{\alpha\beta}^Z$, in the interval $[0-2\pi]$. In both cases, we notice that the determination of $\sin^2 \theta_{23}$ is mostly impacted by the SME coefficients $a_{e\tau}$ and $a_{e\tau}^Z$, while the $(e - \mu)$ and $(\mu - \tau)$ channels have a mild influence on the determination of the atmospheric mixing angle.

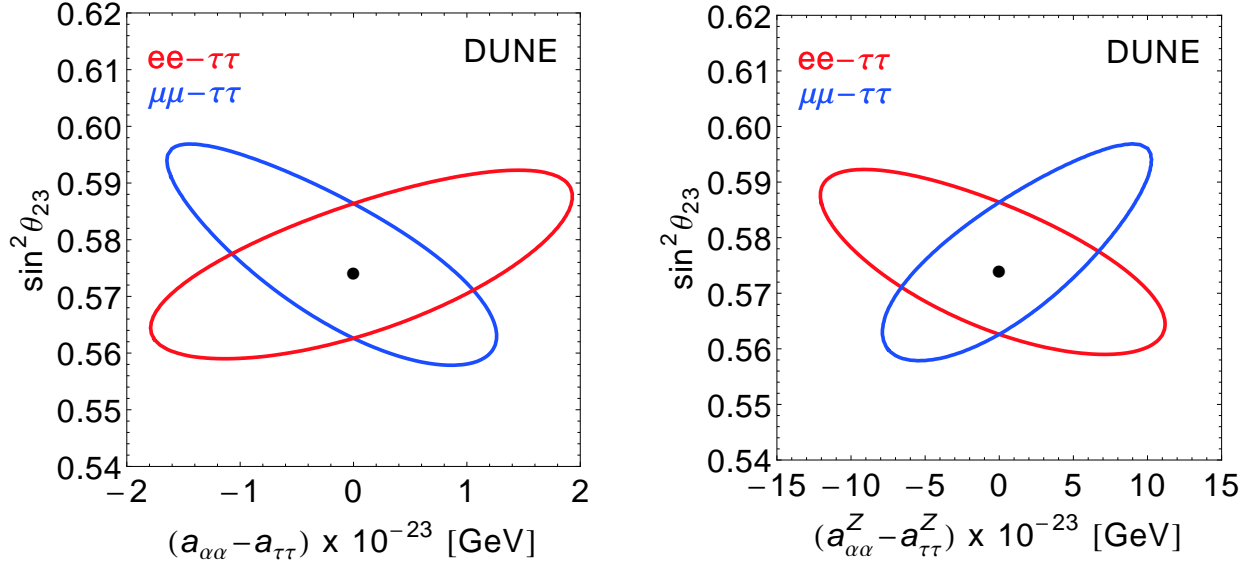


FIG. 6: Expected 95% C.L. sensitivity regions in the $(a_{\alpha\alpha} - a_{\tau\tau}, a_{\alpha\alpha}^Z - a_{\tau\tau}^Z) - \sin^2 \theta_{23}$ projection planes. The (red, blue)-solid lines correspond to $\alpha\alpha = (ee, \mu\mu)$, respectively. We have marginalized over δ_{CP} around its 1σ uncertainty [88]. All the remaining oscillation parameters are fixed to their NO best fit value. See text for a detailed explanation.

In Fig. 6, we observe that the diagonal SME coefficients have a similar impact on the determination of the mixing angle, showing a positive (negative) correlation for the isotropic SME coefficients, $a_{ee} - a_{\tau\tau}$ ($a_{\mu\mu} - a_{\tau\tau}$), and negative (positive) correlation for the Z -spatial ones, $a_{ee}^Z - a_{\tau\tau}^Z$ ($a_{\mu\mu}^Z - a_{\tau\tau}^Z$).

D. Sensitivities and correlations of the LIV phases $(\phi_{\alpha\beta}, \phi_{\alpha\beta}^Z)$ with δ_{CP}

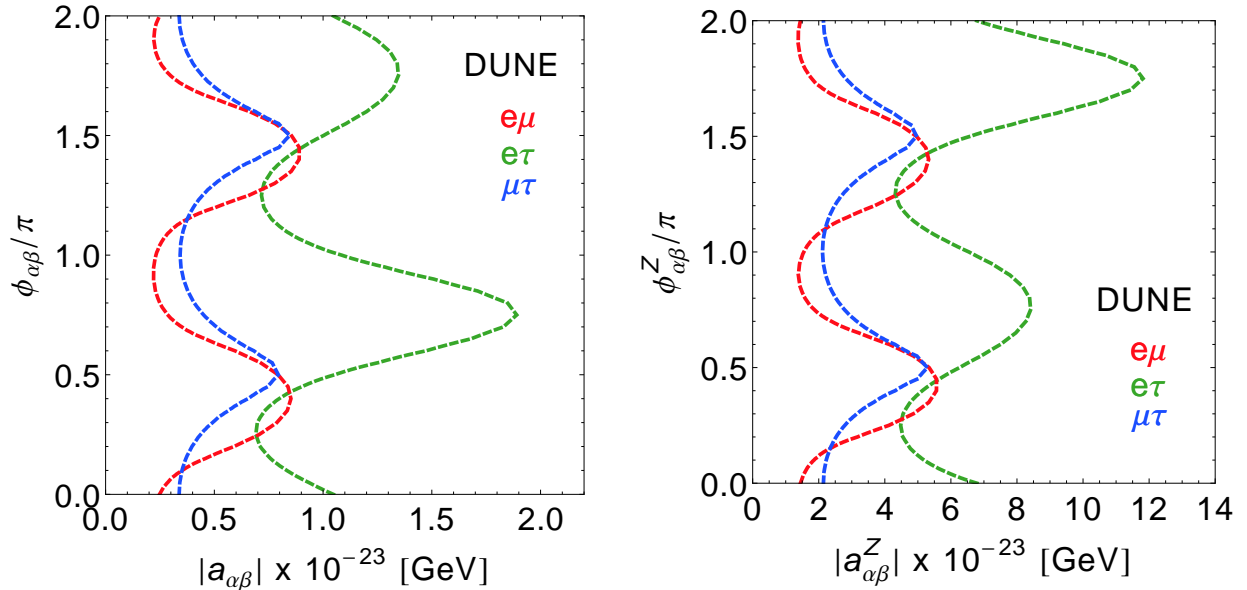


FIG. 7: Expected 95% C.L. sensitivity regions in the $\phi_{\alpha\beta}$ vs. $|a_{\alpha\beta}|$ (left) and $\phi_{\alpha\beta}^Z$ vs. $|a_{\alpha\beta}^Z|$ (right) projection planes. The (red, green, blue)-dashed lines correspond to the SME coefficients from the $\alpha\beta = (e\mu, e\tau, \mu\tau)$ channels, respectively. We marginalize over θ_{23} and δ_{CP} around their 1σ uncertainty [88]. All the remaining oscillation parameters are fixed to their NO best fit value. See text for a detailed explanation.

In Fig. 7, we present our results of the expected sensitivities to the SME coefficients $a_{\alpha\beta}$ and $a_{\alpha\beta}^Z$ at DUNE, the projected 95% C.L. sensitivities to the isotropic SME coefficients are $|a_{e\tau}| \lesssim 1.6 \times 10^{-23}$ GeV, $|a_{e\mu}| \lesssim 0.9 \times 10^{-23}$ GeV, and $|a_{\mu\tau}| \lesssim 0.8 \times 10^{-23}$ GeV, respectively, while for the Z -spatial coefficients, the expected 95% C.L. sensitivities are $|a_{e\tau}^Z| \lesssim 7.8 \times 10^{-23}$ GeV, $|a_{e\mu}^Z| \lesssim 5.7 \times 10^{-23}$ GeV, and $|a_{\mu\tau}^Z| \lesssim 5.2 \times 10^{-23}$ GeV, accordingly.

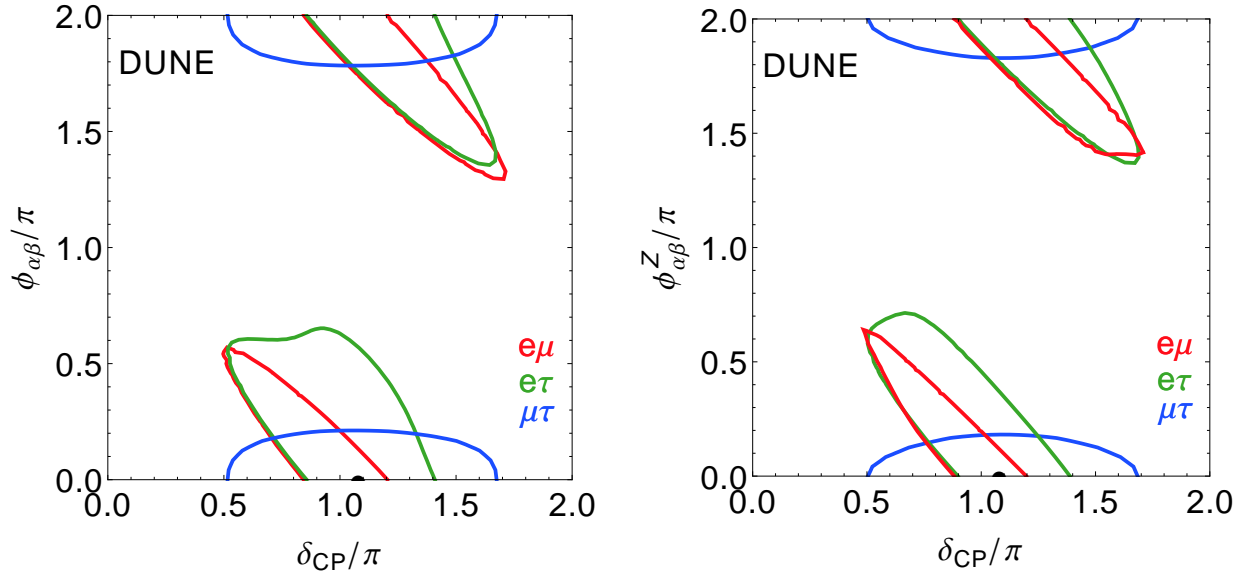


FIG. 8: Expected 95% C.L. sensitivity regions in the $(\phi_{\alpha\beta}, \phi_{\alpha\beta}^Z)$ vs. δ_{CP} – projection planes. The (red, green, blue)-dashed lines correspond to the LIV phases from the $\alpha\beta = (e\mu, e\tau, \mu\tau)$ channels, respectively. We marginalize over θ_{23} around its 1σ uncertainty [88]. The magnitude of the non-diagonal SME coefficients is fixed ($|a_{\alpha\beta}| = 1.0 \times 10^{-23}$ GeV, $|a_{\alpha\beta}^Z| = 8.0 \times 10^{-23}$ GeV). All the remaining oscillation parameters are fixed to their NO best fit value. See text for a detailed explanation.

In Fig. 8, we display the correlations of δ_{CP} with the corresponding LIV phases $\phi_{\alpha\beta}$ and $\phi_{\alpha\beta}^Z$. The magnitude of the non-diagonal SME coefficients were fixed to $|a_{\alpha\beta}| = 1.0 \times 10^{-23}$ GeV and $|a_{\alpha\beta}^Z| = 8.0 \times 10^{-23}$ GeV. We notice that the LIV phases, $\phi_{\alpha\beta}$ and $\phi_{\alpha\beta}^Z$, have a similar impact on the reconstructed δ_{CP} phase. Furthermore, the expected allowed value of the leptonic CP phase is $\delta_{CP}/\pi = 1.08 \pm 0.6$ at 95% C.L. The $(e - \mu)$ and $(e - \tau)$ channels show higher correlations.

V. CONCLUSIONS

High energy neutrino oscillations provide an excellent opportunity to investigate potential breakdowns of the Lorentz and CPT symmetries. In this study, we have analyzed the impact of either the isotropic or anisotropic Z –spatial coefficients for CPT –odd Lorentz violation on the determination of the mixing angle θ_{23} and leptonic CP -phase δ_{CP} , as well as the

projected sensitivities and correlations, considering a DUNE-like setup.

The determination of the aforementioned atmospheric mixing angle θ_{23} and phase δ_{CP} will be mostly impacted by effects from either the isotropic or Z -spatial CPT -odd SME coefficients from the $(e - \tau)$ channel; effects from the $(e - \mu)$ channel are moderate, and the impact from the $(\mu - \tau)$ channel is muted: Figs. 2 and 5. In addition, we observed that the presence of the corresponding LIV phases, $\phi_{\alpha\beta}$ and $\phi_{\alpha\beta}^Z$, will have a similar effect on the reconstructed CP -phase, showing a significant correlation among the flavor-changing channels, $(e - \mu)$ and $(e - \tau)$, accordingly: Fig. 8. Regarding the diagonal elements, $(ee - \tau\tau)$ and $(\mu\mu - \tau\tau)$, the determination of the atmospheric mixing angle θ_{23} will be slightly influenced by the presence of either isotropic or anisotropic coefficients: Fig. 6. Effects from the diagonal $(ee - \tau\tau)$ channel will have a considerable impact on the leptonic CP -phase determination: Fig. 3.

On the other hand, the expected 95% C.L. sensitivities to the isotropic SME coefficients are $|a_{e\tau}| \lesssim 1.6 \times 10^{-23}$ GeV, $|a_{e\mu}| \lesssim 0.9 \times 10^{-23}$ GeV, and $|a_{\mu\tau}| \lesssim 0.8 \times 10^{-23}$ GeV (left panel of Fig. 7), while for the Z -spatial coefficients, the projected 95% C.L. sensitivities are $|a_{e\tau}^Z| \lesssim 7.8 \times 10^{-23}$ GeV, $|a_{e\mu}^Z| \lesssim 5.7 \times 10^{-23}$ GeV, and $|a_{\mu\tau}^Z| \lesssim 5.2 \times 10^{-23}$ GeV, accordingly (right panel of Fig. 7). Besides, we have explored the correlations among the isotropic and Z -spatial sectors (Fig. 1), and limits on the isotropic $a_{\alpha\beta}$ can be relaxed depending on the limits set on the $a_{\alpha\beta}^Z$ coefficients. While current limits set on the $(e - \tau)$ and $(e - \mu)$ channels from the Super-Kamiokande experiment can be improved considering a DUNE-like configuration, that is not the case for the $(\mu - \tau)$ channel, confirming a complementarity between the two experiments.

This paper represents the views of the authors and should not be considered a DUNE collaboration paper.

ACKNOWLEDGEMENTS

We would like to acknowledge J. S. Diaz for useful discussions. This work was partially supported by SNII-México and CONAHCyT research Grant No. A1-S-23238.

Appendix A: DUNE location definitions

In our analysis we consider a fixed value of \hat{N}^Z . Here we show how the value of \hat{N}^Z change in accordance with the determination of the experiment location.

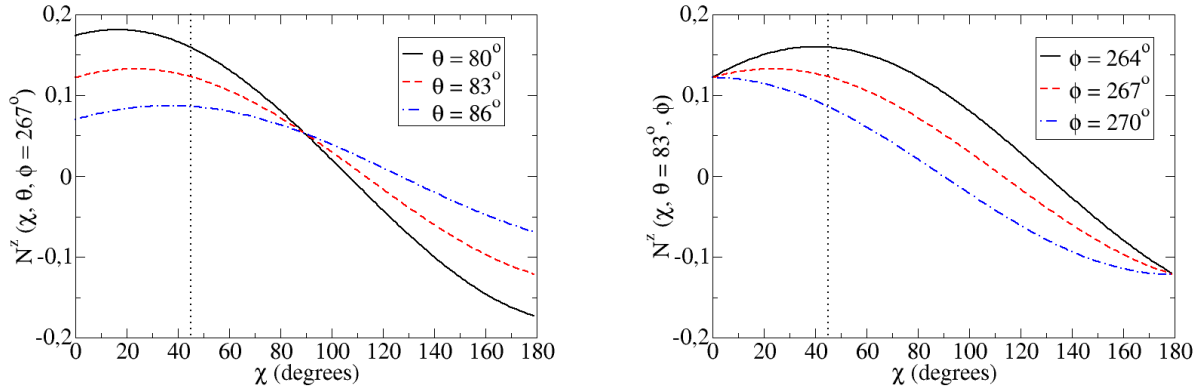


FIG. 9: Values of \hat{N}^Z as a function of χ in degrees. On the left side, $\phi = 267^\circ$ and $\theta = 80^\circ, 83^\circ, 86^\circ$ for black, dashed-red, and dot-dashed-blue lines, respectively. On the right side, $\theta = 83^\circ$ and $\phi = 264^\circ, 267^\circ, 270^\circ$ for black, dashed-red, and dot-dashed-blue lines, respectively. The vertical dotted line indicates the value of $\chi = 45.6^\circ$, used in our analysis.

Parameter	Definition	Value
χ	Colatitude	45.6°
θ	Angle between beam and vertical	84.2°
ϕ	Angle between beam and east of south	262.5°

TABLE II: DUNE beam direction in terms of the Sun-centered frame angle definitions.

As displayed in Fig. 9, and from Eqs. (4) and (5), experiment location resulting in bigger values of \hat{N}^Z could enhance the sensitivity of the Z -spatial SME coefficients $(\tilde{a}_L)_{\alpha\beta}^Z$.

[1] M. A. Acero *et al.* [NOvA], Phys. Rev. D **106** (2022) no.3, 032004
doi:10.1103/PhysRevD.106.032004 [[arXiv:2108.08219](https://arxiv.org/abs/2108.08219) [hep-ex]].

- [2] M. A. Acero *et al.* [NOvA], Phys. Rev. D **110** (2024) no.1, 1 doi:10.1103/PhysRevD.110.012005 [[arXiv:2311.07835](#) [hep-ex]].
- [3] K. Abe *et al.* [T2K], Eur. Phys. J. C **83** (2023) no.9, 782 doi:10.1140/epjc/s10052-023-11819-x [[arXiv:2303.03222](#) [hep-ex]].
- [4] K. Abe *et al.* [T2K], Phys. Rev. D **108** (2023) no.7, 072011 doi:10.1103/PhysRevD.108.072011 [[arXiv:2305.09916](#) [hep-ex]].
- [5] R. Abbasi *et al.* [IceCube], [[arXiv:2405.02163](#) [hep-ex]].
- [6] K. Abe *et al.* [T2K and Super-Kamiokande], [[arXiv:2405.12488](#) [hep-ex]].
- [7] P. B. Denton, J. Gehrlein and R. Pestes, Phys. Rev. Lett. **126** (2021) no.5, 051801 doi:10.1103/PhysRevLett.126.051801 [[arXiv:2008.01110](#) [hep-ph]].
- [8] S. S. Chatterjee and A. Palazzo, Phys. Rev. Lett. **126** (2021) no.5, 051802 doi:10.1103/PhysRevLett.126.051802 [[arXiv:2008.04161](#) [hep-ph]].
- [9] L. A. Delgadillo and O. G. Miranda, Phys. Rev. D **108** (2023) no.9, 095024 doi:10.1103/PhysRevD.108.095024 [[arXiv:2304.05545](#) [hep-ph]].
- [10] S. S. Chatterjee and A. Palazzo, [[arXiv:2005.10338](#) [hep-ph]].
- [11] A. de Gouvêa, G. Jusino Sánchez and K. J. Kelly, Phys. Rev. D **106** (2022) no.5, 055025 doi:10.1103/PhysRevD.106.055025 [[arXiv:2204.09130](#) [hep-ph]].
- [12] H. X. Lin, J. Tang and S. Vihonen, [[arXiv:2312.11704](#) [hep-ph]].
- [13] D. Colladay and V. A. Kostelecky, Phys. Rev. D **58** (1998), 116002 doi:10.1103/PhysRevD.58.116002 [[arXiv:hep-ph/9809521](#) [hep-ph]].
- [14] V. A. Kostelecky and S. Samuel, Phys. Rev. D **39** (1989), 683 doi:10.1103/PhysRevD.39.683
- [15] V. A. Kostelecky and R. Potting, Nucl. Phys. B **359** (1991), 545-570 doi:10.1016/0550-3213(91)90071-5
- [16] V. A. Kostelecky and R. Potting, Phys. Lett. B **381** (1996), 89-96 doi:10.1016/0370-2693(96)00589-8 [[arXiv:hep-th/9605088](#) [hep-th]].
- [17] D. Colladay and V. A. Kostelecky, Phys. Rev. D **55** (1997), 6760-6774 doi:10.1103/PhysRevD.55.6760 [[arXiv:hep-ph/9703464](#) [hep-ph]].
- [18] P. H. Gu, X. J. Bi and X. m. Zhang, Eur. Phys. J. C **50** (2007), 655-659 doi:10.1140/epjc/s10052-007-0217-7 [[arXiv:hep-ph/0511027](#) [hep-ph]].
- [19] S. Ando, M. Kamionkowski and I. Mocioiu, Phys. Rev. D **80** (2009), 123522 doi:10.1103/PhysRevD.80.123522 [[arXiv:0910.4391](#) [hep-ph]].

- [20] F. Simpson, R. Jimenez, C. Pena-Garay and L. Verde, *Phys. Dark Univ.* **20** (2018), 72-77 doi:10.1016/j.dark.2018.04.002 [[arXiv:1607.02515](#) [astro-ph.CO]].
- [21] N. Klop and S. Ando, *Phys. Rev. D* **97** (2018) no.6, 063006 doi:10.1103/PhysRevD.97.063006 [[arXiv:1712.05413](#) [hep-ph]].
- [22] F. Capozzi, I. M. Shoemaker and L. Vecchi, *JCAP* **07** (2018), 004 doi:10.1088/1475-7516/2018/07/004 [[arXiv:1804.05117](#) [hep-ph]].
- [23] Y. Farzan and S. Palomares-Ruiz, *Phys. Rev. D* **99** (2019) no.5, 051702 doi:10.1103/PhysRevD.99.051702 [[arXiv:1810.00892](#) [hep-ph]].
- [24] T. Gherghetta and A. Shkerin, *Phys. Rev. D* **108** (2023) no.9, 9 doi:10.1103/PhysRevD.108.095009 [[arXiv:2305.06441](#) [hep-ph]].
- [25] C. A. Argüelles, K. Farrag and T. Katori, *PoS ICRC2023* (2023), 1415 doi:10.22323/1.444.1415 [[arXiv:2402.18126](#) [hep-ph]].
- [26] C. A. Argüelles, K. Farrag and T. Katori, doi:10.1142/9789811275388_0047 [[arXiv:2401.15716](#) [hep-ph]].
- [27] G. Lambiase and T. K. Poddar, *JCAP* **01** (2024), 069 doi:10.1088/1475-7516/2024/01/069 [[arXiv:2307.05229](#) [hep-ph]].
- [28] R. Cordero and L. A. Delgadillo, *Phys. Lett. B* **853** (2024), 138687 doi:10.1016/j.physletb.2024.138687 [[arXiv:2312.16320](#) [hep-ph]].
- [29] C. A. Argüelles, K. Farrag and T. Katori, [[arXiv:2404.10926](#) [hep-ph]].
- [30] V. A. Kostelecky and M. Mewes, *Phys. Rev. D* **69** (2004), 016005 doi:10.1103/PhysRevD.69.016005 [[arXiv:hep-ph/0309025](#) [hep-ph]].
- [31] A. Kostelecky and M. Mewes, *Phys. Rev. D* **85** (2012), 096005 doi:10.1103/PhysRevD.85.096005 [[arXiv:1112.6395](#) [hep-ph]].
- [32] J. S. Diaz, *Symmetry* **8** (2016) no.10, 105 doi:10.3390/sym8100105 [[arXiv:1609.09474](#) [hep-ph]].
- [33] M. D. C. Torri, *Universe* **6** (2020) no.3, 37 doi:10.3390/universe6030037 [[arXiv:2110.09186](#) [hep-ph]].
- [34] C. A. Moura and F. Rossi-Torres, *Universe* **8** (2022) no.1, 42 doi:10.3390/universe8010042
- [35] G. Barenboim, *Front. in Phys.* **10** (2022), 813753 doi:10.3389/fphy.2022.813753
- [36] H. Murayama and T. Yanagida, *Phys. Lett. B* **520** (2001), 263-268 doi:10.1016/S0370-2693(01)01136-4 [[arXiv:hep-ph/0010178](#) [hep-ph]].

- [37] G. Barenboim, L. Borissoy, J. D. Lykken and A. Y. Smirnov, *JHEP* **10** (2002), 001 doi:10.1088/1126-6708/2002/10/001 [[arXiv:hep-ph/0108199](#) [hep-ph]].
- [38] G. Barenboim and N. E. Mavromatos, *JHEP* **01** (2005), 034 doi:10.1088/1126-6708/2005/01/034 [[arXiv:hep-ph/0404014](#) [hep-ph]].
- [39] V. A. Kostelecky and M. Mewes, *Phys. Rev. D* **70** (2004), 076002 doi:10.1103/PhysRevD.70.076002 [[arXiv:hep-ph/0406255](#) [hep-ph]].
- [40] A. A. Aguilar-Arevalo *et al.* [MiniBooNE], *Phys. Lett. B* **718** (2013), 1303-1308 doi:10.1016/j.physletb.2012.12.020 [[arXiv:1109.3480](#) [hep-ex]].
- [41] T. Katori [MiniBooNE], *Mod. Phys. Lett. A* **27** (2012), 1230024 doi:10.1142/S0217732312300248 [[arXiv:1206.6915](#) [hep-ex]].
- [42] J. N. Bahcall, V. Barger and D. Marfatia, *Phys. Lett. B* **534** (2002), 120-123 doi:10.1016/S0370-2693(02)01714-8 [[arXiv:hep-ph/0201211](#) [hep-ph]].
- [43] Y. Abe *et al.* [Double Chooz], *Phys. Rev. D* **86** (2012), 112009 doi:10.1103/PhysRevD.86.112009 [[arXiv:1209.5810](#) [hep-ex]].
- [44] P. Adamson *et al.* [MINOS], *Phys. Rev. Lett.* **101** (2008), 151601 doi:10.1103/PhysRevLett.101.151601 [[arXiv:0806.4945](#) [hep-ex]].
- [45] P. Adamson *et al.* [MINOS], *Phys. Rev. Lett.* **105** (2010), 151601 doi:10.1103/PhysRevLett.105.151601 [[arXiv:1007.2791](#) [hep-ex]].
- [46] R. Abbasi *et al.* [IceCube], *Phys. Rev. D* **82** (2010), 112003 doi:10.1103/PhysRevD.82.112003 [[arXiv:1010.4096](#) [astro-ph.HE]].
- [47] K. Abe *et al.* [Super-Kamiokande], *Phys. Rev. D* **91** (2015) no.5, 052003 doi:10.1103/PhysRevD.91.052003 [[arXiv:1410.4267](#) [hep-ex]].
- [48] B. Aharmim *et al.* [SNO], *Phys. Rev. D* **98** (2018) no.11, 112013 doi:10.1103/PhysRevD.98.112013 [[arXiv:1811.00166](#) [hep-ex]].
- [49] G. Barenboim, C. A. Ternes and M. Tórtola, *Phys. Lett. B* **780** (2018), 631-637 doi:10.1016/j.physletb.2018.03.060 [[arXiv:1712.01714](#) [hep-ph]].
- [50] G. Barenboim, M. Masud, C. A. Ternes and M. Tórtola, *Phys. Lett. B* **788** (2019), 308-315 doi:10.1016/j.physletb.2018.11.040 [[arXiv:1805.11094](#) [hep-ph]].
- [51] S. Kumar Agarwalla and M. Masud, *Eur. Phys. J. C* **80** (2020) no.8, 716 doi:10.1140/epjc/s10052-020-8303-1 [[arXiv:1912.13306](#) [hep-ph]].
- [52] U. Rahaman, *Eur. Phys. J. C* **81** (2021) no.9, 792 doi:10.1140/epjc/s10052-021-09598-4

- [arXiv:2103.04576 [hep-ph]].
- [53] T. V. Ngoc, S. Cao, N. T. H. Van and P. T. Quyen, Phys. Rev. D **107** (2023) no.1, 016013 doi:10.1103/PhysRevD.107.016013 [arXiv:2210.13044 [hep-ph]].
- [54] A. Sarker, A. Medhi and M. M. Devi, Eur. Phys. J. C **83** (2023) no.7, 592 doi:10.1140/epjc/s10052-023-11785-4 [arXiv:2302.10456 [hep-ph]].
- [55] D. Raikwal, S. Choubey and M. Ghosh, Phys. Rev. D **107** (2023) no.11, 115032 doi:10.1103/PhysRevD.107.115032 [arXiv:2303.10892 [hep-ph]].
- [56] S. Sahoo, A. Kumar and S. K. Agarwalla, JHEP **03** (2022), 050 doi:10.1007/JHEP03(2022)050 [arXiv:2110.13207 [hep-ph]].
- [57] S. K. Agarwalla, S. Das, S. Sahoo and P. Swain, JHEP **07** (2023), 216 doi:10.1007/JHEP07(2023)216 [arXiv:2302.12005 [hep-ph]].
- [58] S. Mishra, S. Shukla, L. Singh and V. Singh, [arXiv:2309.01756 [hep-ph]].
- [59] G. Barenboim, C. A. Ternes and M. Tórtola, Eur. Phys. J. C **79** (2019) no.5, 390 doi:10.1140/epjc/s10052-019-6900-7 [arXiv:1804.05842 [hep-ph]].
- [60] S. Sahoo, A. Kumar, S. K. Agarwalla and A. Dighe, Phys. Lett. B **841** (2023), 137949 doi:10.1016/j.physletb.2023.137949 [arXiv:2205.05134 [hep-ph]].
- [61] R. Majhi, D. K. Singha, M. Ghosh and R. Mohanta, Phys. Rev. D **107** (2023) no.7, 075036 doi:10.1103/PhysRevD.107.075036 [arXiv:2212.07244 [hep-ph]].
- [62] G. Barenboim, P. Martínez-Miravé, C. A. Ternes and M. Tórtola, Phys. Rev. D **108** (2023) no.3, 035039 doi:10.1103/PhysRevD.108.035039 [arXiv:2305.06384 [hep-ph]].
- [63] S. Pan, K. Chakraborty and S. Goswami, Eur. Phys. J. C **84** (2024) no.4, 354 doi:10.1140/epjc/s10052-024-12541-y [arXiv:2308.07566 [hep-ph]].
- [64] C. A. Argüelles, T. Katori and J. Salvado, Phys. Rev. Lett. **115** (2015), 161303 doi:10.1103/PhysRevLett.115.161303 [arXiv:1506.02043 [hep-ph]].
- [65] N. Fiza, N. R. Khan Chowdhury and M. Masud, JHEP **01** (2023), 076 doi:10.1007/JHEP01(2023)076 [arXiv:2206.14018 [hep-ph]].
- [66] R. Cordero and L. A. Delgadillo, [arXiv:2407.02729 [hep-ph]].
- [67] S. Shukla, S. Mishra, L. Singh and V. Singh, [arXiv:2408.01520 [hep-ph]].
- [68] R. Abbasi *et al.* [IceCube], Nature Phys. **18** (2022) no.11, 1287-1292 doi:10.1038/s41567-022-01762-1 [arXiv:2111.04654 [hep-ex]].
- [69] F. Testagrossa, D. F. G. Fiorillo and M. Bustamante, [arXiv:2310.12215 [astro-ph.HE]].

- [70] B. Telalovic and M. Bustamante, [[arXiv:2310.15224](#) [astro-ph.HE]].
- [71] J. S. Díaz, A. Kostelecký and R. Lehnert, Phys. Rev. D **88** (2013) no.7, 071902 doi:10.1103/PhysRevD.88.071902 [[arXiv:1305.4636](#) [hep-ph]].
- [72] R. Lehnert, Phys. Lett. B **828** (2022), 137017 doi:10.1016/j.physletb.2022.137017 [[arXiv:2112.13803](#) [hep-ph]].
- [73] M. Aker *et al.* [KATRIN], Phys. Rev. D **107** (2023) no.8, 082005 doi:10.1103/PhysRevD.107.082005 [[arXiv:2207.06326](#) [nucl-ex]].
- [74] J. B. Albert *et al.* [EXO-200], Phys. Rev. D **93** (2016) no.7, 072001 doi:10.1103/PhysRevD.93.072001 [[arXiv:1601.07266](#) [nucl-ex]].
- [75] O. Azzolini *et al.* [CUPID], Phys. Rev. D **100** (2019) no.9, 092002 doi:10.1103/PhysRevD.100.092002 [[arXiv:1911.02446](#) [nucl-ex]].
- [76] J. S. Diaz and F. R. Klinkhamer, Phys. Rev. D **93** (2016) no.5, 053004 doi:10.1103/PhysRevD.93.053004 [[arXiv:1512.00817](#) [hep-ph]].
- [77] B. Abi *et al.* [DUNE], Eur. Phys. J. C **80** (2020) no.10, 978 doi:10.1140/epjc/s10052-020-08456-z [[arXiv:2006.16043](#) [hep-ex]].
- [78] J. S. Diaz, V. A. Kostelecky and M. Mewes, Phys. Rev. D **80**, 076007 (2009) doi:10.1103/PhysRevD.80.076007 [[arXiv:0908.1401](#) [hep-ph]].
- [79] Q. G. Bailey and V. A. Kostelecky, Phys. Rev. D **74** (2006), 045001 doi:10.1103/PhysRevD.74.045001 [[arXiv:gr-qc/0603030](#) [gr-qc]].
- [80] P. Huber, M. Lindner and W. Winter, Comput. Phys. Commun. **167** (2005), 195 doi:10.1016/j.cpc.2005.01.003 [[arXiv:hep-ph/0407333](#) [hep-ph]].
- [81] P. Huber, J. Kopp, M. Lindner, M. Rolinec and W. Winter, Comput. Phys. Commun. **177** (2007), 432-438 doi:10.1016/j.cpc.2007.05.004 [[arXiv:hep-ph/0701187](#) [hep-ph]].
- [82] J. Kopp, Int. J. Mod. Phys. C **19** (2008), 523-548 doi:10.1142/S0129183108012303 [[arXiv:physics/0610206](#) [physics]].
- [83] J. Kopp, M. Lindner, T. Ota and J. Sato, [[arXiv:0710.1867](#) [hep-ph]].
- [84] B. Abi *et al.* [DUNE], [[arXiv:2103.04797](#) [hep-ex]].
- [85] B. Abi *et al.* [DUNE], JINST **15** (2020) no.08, T08008 doi:10.1088/1748-0221/15/08/T08008 [[arXiv:2002.02967](#) [physics.ins-det]].
- [86] B. Abi *et al.* [DUNE], [[arXiv:2002.03005](#) [hep-ex]].
- [87] P. Huber, M. Lindner and W. Winter, Nucl. Phys. B **645** (2002), 3-48 doi:10.1016/S0550-

3213(02)00825-8 [[arXiv:hep-ph/0204352](#) [hep-ph]].

- [88] P. F. de Salas, D. V. Forero, S. Gariazzo, P. Martínez-Miravé, O. Mena, C. A. Ternes, M. Tórtola and J. W. F. Valle, *JHEP* **02** (2021), 071 doi:10.1007/JHEP02(2021)071 [[arXiv:2006.11237](#) [hep-ph]].